

# Influence of Janus Particle Shape on Their Interfacial Behavior at Liquid–Liquid Interfaces

Thomas M. Ruhland,<sup>†</sup> André H. Gröschel,<sup>†</sup> Nicholas Ballard,<sup>‡</sup> Thomas S. Skelhon,<sup>‡</sup> Andreas Walther,<sup>§</sup> Axel H. E. Müller,<sup>†</sup> and Stefan A. F. Bon\*<sup>‡,§</sup>

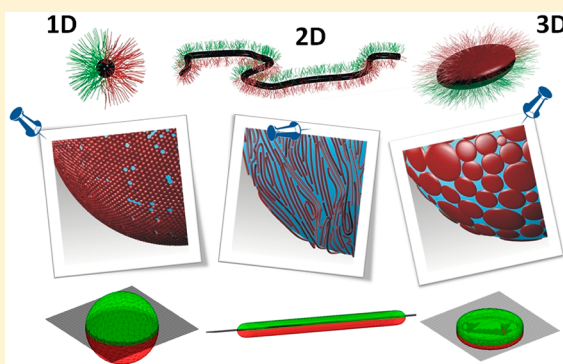
<sup>†</sup>Department of Macromolecular Chemistry II, University Bayreuth, Bayreuth, Germany

<sup>‡</sup>Department of Chemistry, University of Warwick, Coventry CV4 7AL, United Kingdom

<sup>§</sup>DWI at the RWTH Aachen, RWTH Aachen University, 52506 Aachen, Germany

## S Supporting Information

**ABSTRACT:** We investigate the self-assembly behavior of Janus particles with different geometries at a liquid–liquid interface. The Janus particles we focus on are characterized by a phase separation along their major axis into two hemicylinders of different wettability. We present a combination of experimental and simulation data together with detailed studies elucidating the mechanisms governing the adsorption process of Janus spheres, Janus cylinders, and Janus discs. Using the pendant drop technique, we monitor the assembly kinetics following changes in the interfacial tension of nanoparticle adsorption. According to the evolution of the interfacial tension and simulation data, we will specify the characteristics of early to late stages of the Janus particle adsorption and discuss the effect of Janus particle shape and geometry. The adsorption is characterized by three adsorption stages which are based on the different assembly kinetics and different adsorption mechanisms depending on the particle shape.



## INTRODUCTION

One of the most promising research topics in nanotechnology is the bottom-up design of materials via spontaneous self-assembly of desired building blocks. Over the past decades, there have been reports on the self-assembly of a variety of nanosized objects such as nanoparticles, nanorods, or nano-sheets.<sup>1</sup> As a unique type of building block, anisotropic particles, such as patchy, multicompartiment, or Janus particles, have attracted significant interest.<sup>2–4</sup> Over the course of the past few years in particular, Janus particles, named after the double-faced Roman god, have evolved as a very interesting class of very complex internal colloidal structures among micrometer- or nanosized particles<sup>5,6</sup> and therefore have attracted much attention from both industrial and academic areas due to their potential applications in emulsions,<sup>7,8</sup> materials engineering,<sup>9,10</sup> nanoscience,<sup>11</sup> chemical and biological sensors,<sup>12–16</sup> drug delivery, and self-assembly.<sup>17–19</sup> To date, an exciting variety of synthesis methods, assembled structures, and applications are under development with a special focus on polymeric Janus particles.<sup>5,20–22</sup>

Polymeric Janus particles can be divided into several classes according to their architecture and dimensionality. In particular, much attention has been devoted to spherical Janus particles (3D). In contrast, the challenging synthesis of nonspherical Janus particles such as cylinders (1D) and disc-like particles (2D) has so far limited the possibilities for a comprehensive

understanding of their properties. Thus far, only the controlled cross-linking of microphase-segregated structures of block terpolymers is able to produce nanosized Janus spheres, Janus cylinders, and discs on the multigram scale.<sup>20,23–25</sup> Because of this synthetic advantage, the question of understanding their solution and interfacial behavior needs to be answered to find a way to produce new and more efficient materials.

As a result of their noncentrosymmetric architecture, Janus particles uniquely can combine amphiphilicity known from classical molecular surfactants with the Pickering character that strongly holds solid particles at interfaces, effectively by replacing a substantial area of the oil–water interface. This synergy is not accessible for either the chemically homogeneous analogues of the colloidal particles and molecular surfactants. Their superior affinity toward interfaces and their significantly enhanced reduction of interfacial tension as compared to particles with an isotropic chemical makeup<sup>26–28</sup> or classical surfactant molecules<sup>29</sup> raise enormous interest for many technologically relevant real prototype applications as future surfactants and for nanostructuring of interfaces.<sup>21,30</sup>

At the beginning of the past century, Pickering and Ramsden discovered the stabilizing effect of particles in emulsions,<sup>31,32</sup>

**Received:** December 12, 2012

**Revised:** January 10, 2013

**Published:** January 12, 2013

which was followed by the theoretical description of this effect by Pieranski.<sup>33</sup> Nanoparticle adsorption to fluid interfaces has been studied from a fundamental standpoint and exploited in applications.<sup>34–39</sup> Consequently, there is an enormous potential to assemble anisotropic particles as well as Janus particles or anisotropic Janus particles at fluid interfaces. By now, intensive work has been carried out to observe and understand the extraordinarily high adsorption strength of Janus particles at fluid interfaces, driven by the reduction in interfacial energy and the stabilization of liquid–liquid interfaces. In the following, several theoretical and practical studies have been performed to predict Janus particle behavior at liquid–liquid interfaces after Binks and Fletcher's calculations of interfacial adsorption capabilities of biphasic Janus spheres predicted an up to 3-fold stronger adsorption as compared to particles of uniform wettability.<sup>40–44</sup> Additional studies have suggested that the geometry such as their size, aspect ratio, form, and shape as well as the surface properties of Janus particles play a significant role to their surface activity, particle orientation, and packing geometry.<sup>27,26,45–49</sup>

Understanding the effect of Janus particles at fluid interfaces will be critical to find special design criteria for an efficient industrial use of Janus particles. Until now, the importance of controlling the particle shape and form is not so well understood. Nonspherical nanoparticles behave differently at the interfaces due to their shape, and they can show interesting structures and orientation at interfaces.<sup>50–54</sup> The geometry of the particle is a very important factor which governs the adsorbed position. Apart from the interfacial energies, the role of particle size and form and the surface structure are paramount to the gain in the total interfacial energy of the system. Shape is an important parameter in controlling the maximum packing density and, therefore, the surface properties of armored emulsion droplets. The geometry of particles strongly affects their physical properties. Unfortunately, most theoretical work has focused on understanding the behavior of spherical Janus particles, such as their equilibrium orientation, at fluid–fluid interfaces.<sup>40,42,43,48,55,41</sup>

In this article, we present a systematic study on the influence of geometry and shape of polymeric Janus particles on their surface activity and their orientation at a fluid–fluid interface. A combination of simulations and experiments is used to understand in more detail what happens at a toluene–water interface. The effect of Janus cylinders and Janus discs on the interfacial tension of liquid–liquid interfaces (oil/water) was already highlighted in previous studies via the characterization of the time-dependent evolution of the interfacial tensions.<sup>23,26</sup> The Janus particles show a distinct and significant decrease of the interfacial tension as compared to their linear non-cross-linked block terpolymer precursors. Herein, we will deduce the effect of different geometries (spheres, cylinders and discs) on the structures formed at the interface in a direct comparison of these three particle shapes in the same experimental setup for a better understanding of the behavior of Janus particles at liquid–liquid interfaces in order to understand their behavior in more detail and to find the best fields of applications, e.g., as future surfactants. This investigation demonstrates the important role of the particle geometry in the interfacial assembly of the particles.

## ■ EXPERIMENTAL SECTION

**Materials.** All chemicals (p.a. grade) were purchased from Aldrich.

**Synthesis.** Concerning a high control of the particle shape and size, a unique approach based on the self-organization of triblock terpolymers plays a significant role. The synthetic pathway to obtain Janus particles is based on a template-assisted synthesis, involving cross-linking of a bulk film of block terpolymers and a subsequent sonication treatment following the procedure described in the literature.<sup>23,24,56</sup> All polymers used in this paper were synthesized as well as completely characterized in former studies.<sup>23,26,56,57</sup> The subscripts denote the mass fraction in percent as calculated from the <sup>1</sup>H NMR spectrum, and the superscript gives the number-average molecular weight in kg/mol. The two polystyrene-*block*-polybutadiene-*block*-poly(methyl methacrylate) block terpolymers S<sub>41</sub>B<sub>14</sub>M<sub>45</sub><sup>110</sup> (SBM-1, PDI = 1.01) and S<sub>44</sub>B<sub>8</sub>M<sub>48</sub><sup>183</sup> (SBM-2 PDI = 1.05) and the polystyrene-*block*-polybutadiene-*block*-poly(*tert*-butyl acrylate) block terpolymer S<sub>42</sub>B<sub>10</sub>T<sub>48</sub><sup>133</sup> (SBT, PDI = 1.06) used in this study were synthesized via sequential anionic polymerization in tetrahydrofuran (THF) (Table 1).

**Table 1. Correlation of the Block Terpolymer Precursor and the Resulting Janus Particles**

block terpolymer precursor	Janus particle
S <sub>41</sub> B <sub>14</sub> M <sub>45</sub> <sup>110</sup>	Janus cylinders
S <sub>44</sub> B <sub>8</sub> M <sub>48</sub> <sup>183</sup>	Janus spheres
S <sub>42</sub> B <sub>10</sub> T <sub>48</sub> <sup>133</sup>	Janus discs

**Characterization.** Pendant drop tensiometer isotherms of the interfacial tension at the toluene/water interface were measured on a Krüss DSA100 tensiometer at room temperature. The setup of the pendant drop apparatus is shown elsewhere.<sup>58</sup> Computer automation allowed rapid acquisition of the drop image, edge detection, and fitting of the Laplace–Young equation to determine the interfacial tension. We performed the measurements with a degassed Milli-Q-water droplet saturated with toluene immersed in a toluene solution of the Janus particles saturated with water.

Bright-field TEM was performed on Zeiss CEM 902 and LEO 922 OMEGA electron microscopes operated at 80 and 200 kV, respectively. Data evaluation and processing was carried out with Soft Imaging Viewer, Digital Micrograph 365 Demo software, and ImageJ.

**Free Energy Simulations of Janus Particles at a Toluene/Water Interface.** To have a closer look into the adsorption mechanism and particle orientations at the interface, we used a calculation of the free energy profile of a particle orientation in respect to the toluene/water interface in the same way as we already reported.<sup>52</sup> Briefly, we define mathematically the shape of a superellipsoid by

$$\left( \frac{x^{2/n_2}}{r_x} + \frac{y^{2/n_2}}{r_y} \right)^{n_2/n_1} + \frac{z^{2/n_1}}{r_z} = 1$$

where  $x$ ,  $y$ , and  $z$  are Cartesian coordinates.  $r_x$ ,  $r_y$ , and  $r_z$  are the particles  $x$ ,  $y$ , and  $z$  radii, respectively.  $n_1$  and  $n_2$  act as the “squareness” parameters in the  $z$ -axis and the  $xy$ -plane respectively, with  $0 < n_1, n_2 < \infty$ . The particle is constructed from a series of point that satisfy the above equation using a triangular tessellation scheme that connects the points to create a surface. The free energy of adhesion ( $\Delta G_{ad}$ ) for the particle at the interface is calculated similarly to the method used by Pieranski at a series of rotations and translations through the interface from the equation

$$\Delta G_{ad} = \sum_p A_{p1}\gamma_{p1} + \sum_p A_{p2}\gamma_{p2} - A_{12}\gamma_{12}$$

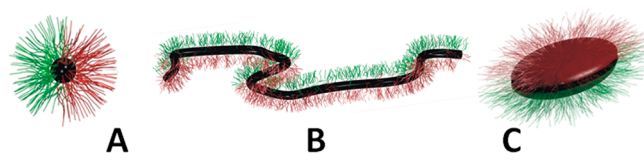
where  $A$  represents area and  $\gamma$  the interfacial tension and the subscripts P1, P2, and 12 correspond to the polymer phases in liquid 1, the polymer phases in liquid 2, and the liquid–liquid interface. The values of the areas are calculated by simply summing the area of triangles of the PMMA or PS phase in the corresponding liquid phase. We

accurately describe the areas by subdividing any triangles that lie at the interface as described in Dijkstra et al.<sup>59</sup> The axis of rotation is along the  $z$ -axis and is performed in the  $xy$ -plane. The translation through the interface is described by a parameter  $Z$  that is given by  $z_{\text{int}}/R_{\text{bound}}$ , where  $z_{\text{int}}$  is the distance from the center of the particle to the liquid–liquid interface and  $R_{\text{bound}}$  is the minimum radius of a sphere that contains all the points given by the equation for a superellipsoid (where  $Z = 1$  the particle resides in the upper liquid phase and where  $Z = -1$  the particle resides in the lower liquid phase). For our simulations we use the data presented in Supporting Information Tables S1 and S2.

## RESULTS AND DISCUSSION

We synthesized three Janus particles with different geometries to isolate the role of shape in the interfacial assembly process. To establish the effect of the Janus character together with the effect of particle shape on the interfacial activity and orientation of the Janus particles at an oil–water interface, we study the influence of Janus spheres, Janus cylinders, and Janus discs, trapped at a toluene/water interface, on the interfacial tension of the system. The geometries of Janus particles used in this study are shown in Scheme 1. Additionally, to understand in

**Scheme 1. Overview of Possible Janus Particle Architectures: (A) Spheres, (B) Cylinders, and (C) Discs**



more detail what happens at the interface, we present simulations about the orientation of the different shaped particles at the liquid–liquid interface to show how geometry influences the strength of the particle adsorption. In order to compare the influence of the geometry, all types of Janus particles were investigated in the same solvent system and under the same conditions.

In pendant drop tensiometry the interfacial tension  $\gamma$  between two immiscible fluids is measured by imaging a pendant droplet of one fluid phase immersed in the second one. The drop profile is automatically detected and fitted with the Young–Laplace equation, extracting the value of  $\gamma$ . An initially relatively high interfacial tension between two completely immiscible fluids is additionally beneficial to

produce a large driving force for the particles to assemble at the interface. In our case water droplets are formed in toluene which contains the dissolved Janus particles and the interfacial tension is measured as a function of time. Adsorption of particles at the liquid–liquid interface lowers the system free energy which translates into an effective interfacial tension reduction; therefore, by monitoring  $\gamma$  as a function of time, we can obtain information about the adsorption kinetics. For the chosen toluene/water interface the determined interfacial tension of the pristine system (34 mN/m) agrees well with the literature value (Supporting Information, Figure 1).<sup>60</sup>

We first studied time-dependent measurements at the toluene/water interface for Janus spheres, Janus discs, and Janus cylinder dissolved in toluene at a concentration of 1 g/L. Figure 1 presents the dynamic surface tension plots and the logarithmic representation of these values, where the interfacial tension decreases with time, approaching a quasi-equilibrium value.

For all particles in the early stages, the interfacial tension drops rapidly because of instantaneous assembly of the particles at the interface, then the decrease in interfacial tension slows down, and once the droplet is mostly covered, the decrease in interfacial tension reaches a quasi-equilibrium. After reaching the plateau value, the Janus particles are located and arranged at the interface. A change in shape of the Janus particles leads to a different adsorption behavior at the interface. We observe different adsorption dynamics for spheres, cylinders, and discs.

The addition of Janus cylinder results in the maximum reduction in the equilibrium interfacial tension. After the addition the interfacial tension between toluene and water is decreased from 34 to ca. 14 mN/m. In comparison, Janus spheres show a moderately lower surface activity with an intermediate  $\gamma_{\infty}$  value of ca. 17.5 mN/m. Janus discs provide the smallest amount of effective interfacial tension reduction. The interfacial tensions decreases from 34 to ca. 19 mN/m. In the case of Janus discs, in addition to a similar trend of adsorption, we observed an additional behavior. The interfacial tension first decreased rapidly, but not so fast as for Janus spheres or Janus cylinders, but slowed down for an extended period of time and finally slowly decreased again until the interfacial tension reached an equilibrium value. After 2 h the interfacial tension reached a plateau around 20.5 mN/m. The next transition occurred after  $2^{1/2}$  h, whereupon the interfacial tension further decreased to an equilibrium interfacial tension ( $\sim 19$  mN/m). This behavior was only observed for the disc-

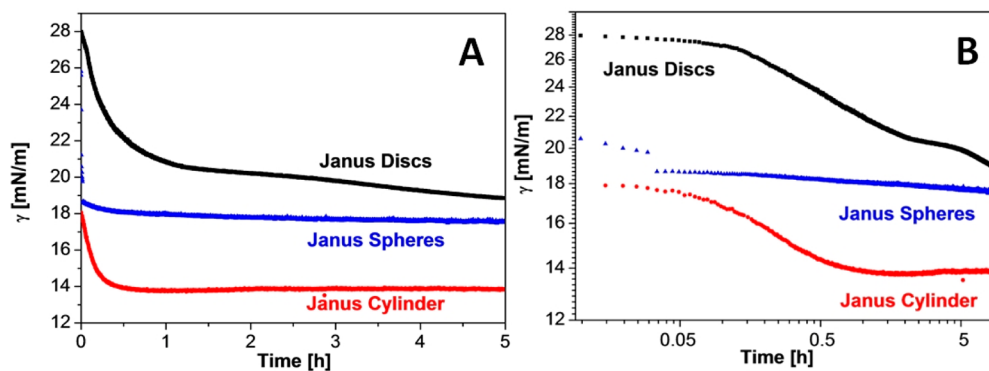


**Figure 1.** Influence of the Janus particle shape on the interfacial tension. (A) Interfacial tension isotherms of solutions of Janus particles in toluene at a water/toluene interface. (B) Logarithmic representation of the data in (A).



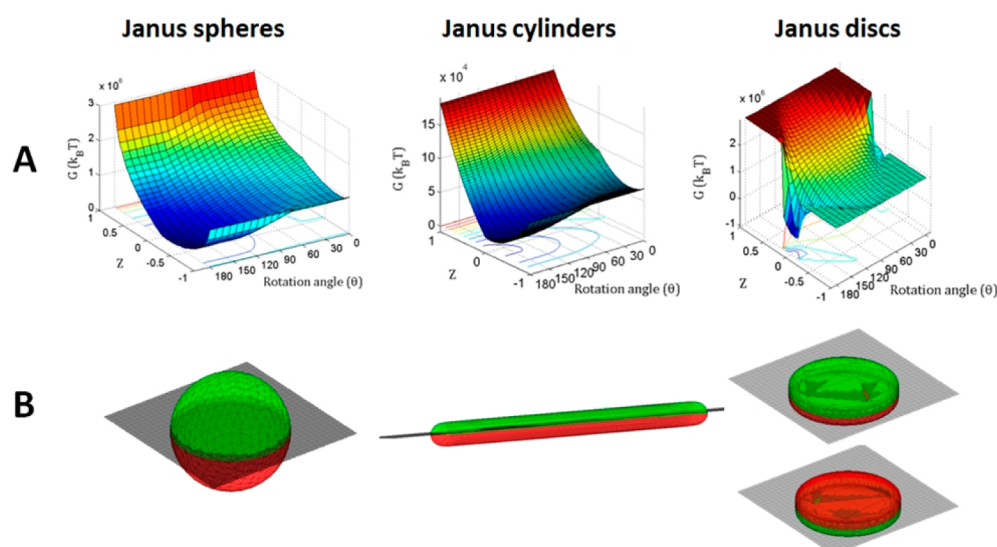


**Figure 2.** (A) Energy profiles for Janus spheres, Janus cylinders, and Janus discs at toluene/water interface. (B) Shape-dependent equilibrium position of Janus particles at toluene (bottom phase) and water (top phase) interface. PS is red labeled, and PMMA is green labeled.

shaped Janus particles, which clearly points toward a change in the packing of the Janus discs at the interface with time due to the anisotropic shape. Furthermore, this indicates that the concentration of particles trapped at the interface influences the packing of Janus discs in a way that is different from Janus spheres, where only a simple decay was observed.

**Comparison and Explanation of Different Adsorption Behavior.** One reason for the different adsorption kinetics is the size of the Janus particles. The Janus spheres are 50 nm in diameter, whereas the cylinders have a length of 2300 nm and the discs are around 300 nm (Supporting Information, Figure S1). Smaller sizes lead to higher diffusion coefficients (Brownian behavior) and thus faster adsorption kinetics. A faster diffusion may also contribute to the lower values of the quasi-equilibrium state as the further minimization in this stage is collision-controlled in contrast to diffusion control in the early stages. Thus, the Janus spheres show a very fast adsorption behavior in the early stages of the process which is completely different to the ones for discs and cylinders. Janus cylinders and Janus discs show slower adsorption kinetics but show a similar initial drop in interfacial tension. Both are highly anisotropic particles and have two length scales, thickness  $h$  and lateral size. A cluster of amphiphilic discs trapped at the interface is equivalent to a closed packing of amphiphilic spheres but without the interstitial space between the different domains filled. Furthermore, domains built up with larger and smaller discs in diameter result in larger interstitial spaces compared with domains with monodisperse spheres. Upon adsorption, Janus cylinders show differences in their structure when compared with those of spherical ones. Probably, this is due to the fact that cylindrical particles can easily slide along their long axis and built up more dense domains. All results confirm our experimental observation that all Janus particles demonstrate significantly enhanced surface activity but possess different adsorption kinetics resulting from differences in interface stabilization. The ability for stabilization slightly decreases from Janus cylinders to Janus spheres to Janus discs. In order to further understand the absorption behavior and kinetics of Janus particles at liquid–liquid interfaces, we simulated the free energy change upon adsorption of the various types of Janus particles used in this work.

## SIMULATIONS

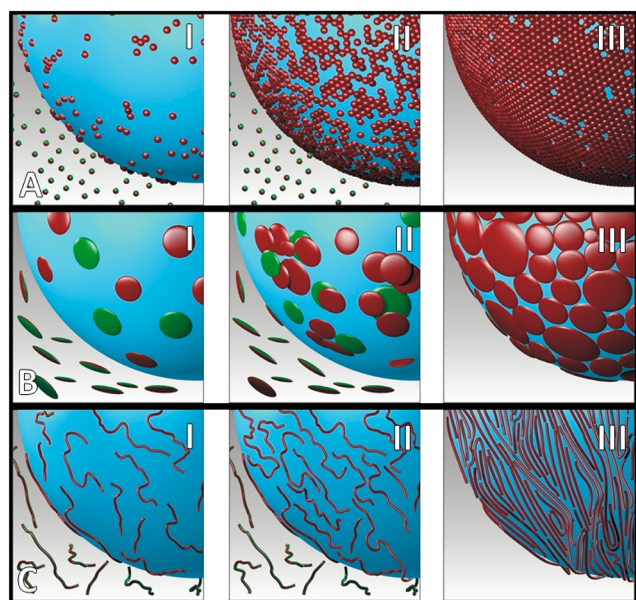
On the basis of the energy profiles, it can generally be seen that Janus particle adsorption is effectively irreversible, because of the depths of the wells in the energy landscapes (Figure 2A). All calculation are based on the particle dimensions mentioned in Tables S1 and S2 representing values determined via TEM, DLS, and AFM. Measurements with the pendant drop tensiometer result in a global interfacial tension which is a function of the packing of the particles and the energy calculated here. In principle, large lateral sized particles offer strong adsorption toward the interface, preventing its removal. Thus, particles with a large cross-sectional area can be strongly adsorbed to the interface. That is the reason for the different energy landscapes of Janus spheres, Janus cylinders, and Janus discs. On the basis of calculated data, we find a favored orientation of polystyrene (PS) to the toluene phase and the poly(methyl methacrylate) (PMMA) side chains to the water phase (Figure 2B).

The energy profile of an isolated Janus sphere at the toluene/water interface indicates one energy minimum with the PS in the toluene phase and the PMMA sitting predominantly in the aqueous phase. The energy barrier for the removal from the interface is  $\sim 5 \times 10^4 kT$ . In comparison, the energy profile of Janus discs indicates two energy minima and therefore predicts the existence of two different orientations of the Janus discs at the toluene/water interface. In the first orientation, the global minimum, the discs are immersed in the toluene phase with their PMMA side just protruding into the aqueous phase, and in the other they are lying upside down with respect to the global minimum, that is, with the PS phase just protruding into the aqueous phase. The energy barrier for removal from the global minimum is  $\sim 1.5 \times 10^6 kT$ , whereas the energy barrier for removal of the second local energy minimum is  $5 \times 10^5 kT$ . Janus cylinders have one energy global minimum. The energy necessary to remove a cylindrical-shaped Janus particle from its equilibrium position at the oil–water interface along is defined as  $1 \times 10^6 kT$ . Janus cylinders are expected to lie with the PS in the toluene phase and the PMMA in the aqueous part and remain oriented parallel to the interface.

On the basis of the experimental data and these simulation results, we can describe the fundamental aspects of Janus particle adsorption and kinetics at liquid–liquid interfaces.

**Mechanism of Janus Particle Adsorption.** As previously mentioned, all particles exhibit different kinetic behaviors due to a different adsorption and packing behavior. Minimal changes in the geometry directly influence the interfacial behavior. The variation in interfacial tension with different particles can be explained by the effect of their geometry on their assembly at the oil/water interface. We now will discuss the fundamental mechanism for each particle geometry in more detail. Additionally, for simplicity we try to come up with a schematic presentation of the different adsorption stages during the adsorption process explaining the adsorption mechanism described below (Scheme 2).

**Scheme 2. Schematic Representation of the Packing Behavior of the Janus Particles at the Toluene/Water Interface during the Adsorption Process<sup>a</sup>**



<sup>a</sup>The most typical adsorption stages pointed out for (A) Janus spheres, (B) Janus discs, and (C) Janus cylinders. The Janus particles are simplified for a better illustration of their position at the liquid–liquid interface (Scheme S1).

**Janus Spheres.** The Janus spheres show a homogeneous size distribution with 50 nm in diameter (Figure S1A). First, the interfacial tension rapidly decreases due to fast Brownian diffusion and adhesion of isolated spheres to the interface (Scheme 2A-I). Subsequently, the decrease in interfacial tension slows down dramatically, as the fraction of unoccupied toluene–water interface becomes limited, preventing successful adhesion upon collision. The particles at the interface pack closer into ordered domains, the domains consist of well-separated and highly ordered individual spheres (Scheme 2A-II), and, finally, minimal packing issues start to dominate and a small decrease in interfacial tension occurs until the assembly attains a quasi-equilibrium. Under these conditions the maximum coverage of the interface with spheres is reached (Scheme 2A-III). The packing of the spheres at the interface is nearly perfect, and in the end, only minimal changes and rearrangements of single spheres take place in order to get the

maximal possible packing. As a result of this, the logarithmic presentation of the interfacial values over time (Figure 1B and Figure S3C) show two stages: a fast decrease in the interfacial tension as a result of diffusion-controlled collision of the particles to the interface and a second slow decrease due to increased packing density and collision-controlled adsorption.

**Janus Discs.** The Janus discs possess a broad size distribution, which is typically obtained at short sonication times. It contains a fraction of relatively large Janus discs with a diameter of 350 nm and fraction of smaller ones with a diameter around 250 nm (Figure S1B). Scheme 2B illustrates the adsorption process for the Janus discs which shows significant differences in comparison to the adsorption of Janus spheres and discs.

Simulation results have suggested that Janus discs of the type used experimentally here have two energy minima at liquid–liquid interfaces. In the early stages of adsorption the adhesion of the Janus discs to the interface is diffusion controlled, and the orientation of the Janus discs upon approach is likely to be random resulting in a roughly bimodal distribution of the two orientations of the particles at the interface (Scheme 2B-I). Exchange between the two orientations and/or removal of the particles in the secondary energy minimum from the interface is unlikely at short time scales because of the large energy involved in the transition. Therefore, there will exist a large proportion of the less energetically favorable orientation in the initial stages and the global interfacial tension value is likely to decrease to a lesser extent than in the cases of Janus spheres or cylinders. This indeed is clearly observed in Figure 1. As the packing density increases, leading to monolayer rafts of aggregated and packed discs and reaches a maximum the value of  $\gamma(t)$  reaches a plateau after 2.0 h (Scheme 2B-II). These dense aggregates collide at their edges and “touch” each other. The collision of the edges can lead to a partial overlap, as thinking analogy compare these rafts with the earths tectonic plates. Movement can cause ridges and trenches which potentially can lead to the formation of a bilayer of discs and/or desorption of discs. Discs with their orientation corresponding to the secondary minimum are more likely to desorb. In contrast to the case of a particle with a single energy minima readorption of particles into the lower global energy minima results in a net lowering of the global interfacial tension, and hence a period of slow decline in the global interfacial tension occurs corresponding to the slow reorientation of particles into the more favored orientation assuming an optimal packing at the interface to avoid edge to edge overlapping or tilted orientations. As a second possibility, discs with the polystyrene phase exposed to the water phase can be covered up through adhesion of a particle on top in the correct conformation. This is an additional point explaining slow dynamics as adhesion of the second must be kinetically slower as collision needs to find a disc with the wrong side up already.

At a given point, particle rearrangements are no longer possible, no free space is left at the interface, and a monolayer system is built up (Scheme 2B-III). Additionally, it is known according to the theory of Nonomura et al.<sup>43</sup> that the largest discs adsorb most strongly. Thus, the polydispersity can be another issue in the adsorption process.

**Janus Cylinders.** Ruhland et al. already presented detailed studies of the interfacial self-assembly of slightly amphiphilic 2300 nm long Janus cylinders (Figure S1C) in a recent work.<sup>26</sup> All results found for particles at a PFO/dioxane and a PFO/

DMSO interface can be transferred and confirmed using a toluene/water interface. The interfacial tension decreases with time and the adsorption process is characterized by three different adsorption stages. In the beginning, free diffusion to the interface occurs (Scheme 2C-I), followed by continuous adsorption of cylinders including ordering and domain formation at the interface (Scheme 2C-II). Finally, additional packing leads to a rearrangement of the domains and to the formation of a multilayer system. The cylinders show a liquid crystalline like short-range correlation at the fluid interfaces (Scheme 2C-III). The logarithmic data point toward a more gradual transition from stage I to II as it can be seen for spheres (Figure S3D). This suggests that the structural rearrangements in the monolayers containing cylindrical particles differ from the case of spheres. In the second stage of adsorption domains with both tip–tip and side–side contacts can be found. Upon adsorption, monolayers show differences in their structure when compared with those of spherical ones. Probably, this is due to the fact that cylindrical particles can easily slide along their long axis, whereas translation in the perpendicular direction and rotation are restricted. The Janus cylinders remain oriented parallel to the interface, and their flexibility allows anchoring of a second, loosely bound Janus cylinder. Furthermore, the particles pack more densely due to in-plane and out-of-plane rearrangements. The local ordering leads to a better packing because of excluded volume interactions, which will increase with increasing aspect ratio.

## CONCLUSION

We have studied the behavior of slightly amphiphilic Janus particles at a liquid–liquid toluene/water interface. The mechanism of particle adsorption was investigated in detail using time-dependent measurements of the interfacial tension via a pendant drop tensiometer. The differences in the reduction of interfacial tension were attributed to enhanced adsorption of Janus particles at the oil–water interface under the influence of different geometries of the Janus particles. Janus spheres, Janus cylinders, and Janus discs show significantly enhanced surface activity as compared to homogeneous particles as shown in previous studies. One interesting point is if the particle geometry and shape plays a crucial role in the interfacial behavior or not. These studies demonstrate based on experiments and simulations that changes in the geometry of the particles strongly influence the stabilizing of the liquid–liquid interface. As the shape changes from spheres to discs and cylinders, you can find different adsorption kinetics, different packing behaviors, different energy barriers, and finally different equilibrium values for the interfacial tension. Notably, the dynamic interfacial behaviors of the particles are governed by the packing behavior at the interface, which set the energy barrier for their adsorption. The interfacial tension depends not only on length and concentration of the particles but also on their form and shape and on the packing behavior of the Janus particles. On the basis of that, the adsorption behavior is characterized by different adsorption steps, which show similar trends but differ in detail. The combination of experimental data and modeling results lends itself to the discussion of several interesting issues. It is a noteworthy fact that our very simple simulation approach explains several qualitative features of our experiments. Given the important role that the interfacial assembly of particles plays in the formation and stability of droplets, these studies provide

useful guidelines for designing particles for interfacial stabilization.

## ASSOCIATED CONTENT

### Supporting Information

Figures S1–S3, Scheme S1, and Tables S1, S2. This material is available free of charge via the Internet at <http://pubs.acs.org>.

## AUTHOR INFORMATION

### Corresponding Author

\*E-mail [S.Bon@warwick.ac.uk](mailto:S.Bon@warwick.ac.uk).

### Notes

The authors declare no competing financial interest.

## ACKNOWLEDGMENTS

This work was supported by DFG within SFB 840 (project A1). The authors thank André H. Gröschel for his help with the schemes and Dr. Andreas Walther for providing the Janus discs and for fruitful discussions. Thomas Ruhland thanks the Bavarian Elite Support Program (ENB) for a scholarship. Part of the equipment used in this research was obtained through Birmingham Science City: Innovative Uses for Advanced Materials in the Modern World (West Midlands Centre for Advanced Materials Project 2), with support from Advantage West Midlands (AWM) and part funded by the European Regional Development Fund (ERDF).

## REFERENCES

- (1) Glotzer, S. C.; Solomon, M. J. Anisotropy of Building Blocks and Their Assembly into Complex Structures. *Nat. Mater.* **2007**, *6*, 557–562.
- (2) Loget, G.; Kuhn, A. Bulk Synthesis of Janus Objects and Asymmetric Patchy Particles. *J. Mater. Chem.* **2012**, *22*, 15457–15474.
- (3) Chen, Q.; Yan, J.; Zhang, J.; Bae, S. C.; Granick, S. Janus and multiblock colloidal particles. *Langmuir* **2012**, *28*, 13555–13561.
- (4) Du, J.; O'Reilly, R. K. Anisotropic Particles with Patchy, Multicompartment and Janus Architectures: Preparation and Application. *Chem. Soc. Rev.* **2011**, *40*, 2402–2416.
- (5) Walther, A.; Müller, A. H. E. Janus Particles. *Soft Matter* **2008**, *4*, 663–668.
- (6) Hong, L.; Jiang, S.; Granick, S. Simple Method to Produce Janus Colloidal Particles in Large Quantity. *Langmuir* **2006**, *22*, 9495–9499.
- (7) Walther, A.; Hoffmann, M.; Müller, A. H. E. Emulsion Polymerization Using Janus Particles As Stabilizers. *Angew. Chem., Int. Ed.* **2008**, *47*, 711–714.
- (8) Kim, J.-W.; Lee, D.; Shum, H. C.; Weitz, D. A. Colloid Surfactants for Emulsion Stabilization. *Adv. Mater.* **2008**, *20*, 3239–3243.
- (9) Perro, A.; Reculosa, S.; Ravaine, S.; Bourgeat-Lami, E.; Duguet, E. Design and Synthesis of Janus Micro- and Nanoparticles. *J. Mater. Chem.* **2005**, *15*, 3745–3760.
- (10) Erb, R. M.; Jenness, N. J.; Clark, R. L.; Yellen, B. B. Towards Holonomic Control of Janus Particles in Optomagnetic Traps. *Adv. Mater.* **2009**, *21*, 4825–4829.
- (11) de Gennes, P.-G. Soft Matter (Nobel Lecture). *Angew. Chem., Int. Ed.* **1992**, *31*, 842–845.
- (12) Faria, J.; Ruiz, M. P.; Resasco, D. E. Phase-Selective Catalysis in Emulsions Stabilized by Janus Silica-Nanoparticles. *Adv. Synth. Catal.* **2010**, *352*, 2359–2364.
- (13) Behrend, C. J.; Anker, J. N.; Kopelman, R. Brownian Modulated Optical Nanoprobes. *Appl. Phys. Lett.* **2004**, *84*, 154–156.
- (14) Behrend, C. J.; Anker, J. N.; McNaughton, B. H.; Brasuel, M.; Philbert, M. A.; Kopelman, R. Metal-Capped Brownian and Magnetically Modulated Optical Nanoprobes (MOONs): Micromechanics in Chemical and Biological Microenvironments. *J. Phys. Chem. B* **2004**, *108*, 10408–10414.



- (15) Kaufmann, T.; Gokmen, M. T.; Wendeln, C.; Schneiders, M.; Rinnen, S.; Arlinghaus, H. F.; Bon, S. A. F.; Du Prez, F. E.; Ravoo, B. J. "Sandwich" Microcontact Printing as a Mild Route Towards Monodisperse Janus Particles with Tailored Bifunctionality. *Adv. Mater.* **23**, 79–83.
- (16) Nisisako, T.; Torii, T.; Takahashi, T.; Takizawa, Y. Synthesis of Monodisperse Bicolored Janus Particles with Electrical Anisotropy Using a Microfluidic Co-Flow System. *Adv. Mater.* **2006**, *18*, 1152–1156.
- (17) Jiang, S.; Chen, Q.; Tripathy, M.; Luijten, E.; Schweizer, K. S.; Granick, S. Janus Particle Synthesis and Assembly. *Adv. Mater.* **2010**, *22*, 1060–1071.
- (18) Whitelam, S.; Bon, S. A. F. Self-Assembly of Amphiphilic Peanut-Shaped Nanoparticles. *J. Chem. Phys.* **2010**, *132*, 74901–74908.
- (19) Hong, L.; Cacciuto, A.; Luijten, E.; Granick, S. Clusters of Charged Janus Spheres. *Nano Lett.* **2006**, *6*, 2510–2514.
- (20) Walther, A.; Drechsler, M.; Rosenfeldt, S.; Harnau, L.; Ballauff, M.; Abetz, V.; Müller, A. H. E. Self-Assembly of Janus Cylinders into Hierarchical Superstructures. *J. Am. Chem. Soc.* **2009**, *131*, 4720–4728.
- (21) Wurm, F.; Kilbinger, A. F. M. Polymeric Janus Particles. *Angew. Chem., Int. Ed.* **2009**, *48*, 8412–8421.
- (22) Gröschel, A. H.; Walther, A.; Löbbling, T. I.; Schmelz, J.; Hanisch, A.; Schmalz, H.; Müller, A. H. E. Facile, Solution-Based Synthesis of Soft, Nanoscale Janus Particles with Tunable Janus Balance. *J. Am. Chem. Soc.* **2012**, *134*, 13850–13860.
- (23) Walther, A.; Andre, X.; Drechsler, M.; Abetz, V.; Müller, A. H. E. Janus Discs. *J. Am. Chem. Soc.* **2007**, *129*, 6187–6198.
- (24) Liu, Y.; Abetz, V.; Müller, A. H. E. Janus Cylinders. *Macromolecules* **2003**, *36*, 7894–7898.
- (25) Wolf, A.; Walther, A.; Müller, A. H. E. Janus Triad: Three Types of Nonspherical, Nanoscale Janus Particles from One Single Triblock Terpolymer. *Macromolecules* **2011**, *44*, 9221–9229.
- (26) Ruhland, T. M.; Gröschel, A. H.; Walther, A.; Müller, A. H. E. Janus Cylinders at Liquid–Liquid Interfaces. *Langmuir* **2011**, *27*, 9807–9814.
- (27) Glaser, N.; Adams, D. J.; Böker, A.; Krausch, G. Janus Particles at Liquid–Liquid Interfaces. *Langmuir* **2006**, *22*, 5227–5229.
- (28) Walther, A.; Matussek, K.; Müller, A. H. E. Engineering Nanostructured Polymer Blends with Controlled Nanoparticle Location using Janus Particles. *ACS Nano* **2008**, *2*, 1167–1178.
- (29) Binks, B. P. Particles as Surfactants - Similarities and Differences. *Curr. Opin. Colloid Interface Sci.* **2002**, *7*, 21–41.
- (30) Pawar, A. B.; Kretschmar, I. Fabrication, Assembly, and Application of Patchy Particles. *Macromol. Rapid Commun.* **2010**, *31*, 150–168.
- (31) Pickering, S. U. CXCVI-Emulsions. *J. Chem. Soc., Trans.* **1907**, *91*, 2001–2021.
- (32) Ramsden, W. Separation of Solids in the Surface-Layers of Solutions and "Suspensions" (Observations on Surface-Membranes, Bubbles, Emulsions, and Mechanical Coagulation). *Proc. R. Soc. London* **1903**, *72*, 156–164.
- (33) Pieranski, P. Two-Dimensional Interfacial Colloidal Crystals. *Phys. Rev. Lett.* **1980**, *45*, 569–572.
- (34) Niu, Z.; He, J.; Russell, T. P.; Wang, Q. Synthesis of Nano/Microstructures at Fluid Interfaces. *Angew. Chem., Int. Ed.* **2010**, *49*, 10052–10066.
- (35) Garbin, V.; Crocker, J. C.; Stebe, K. J. Nanoparticles at Fluid Interfaces: Exploiting Capping Ligands to Control Adsorption, Stability and Dynamics. *J. Colloid Interface Sci.* **2012**, *387*, 1–11.
- (36) Lewandowski, E. P.; Bernate, J. A.; Searson, P. C.; Stebe, K. J. Rotation and Alignment of Anisotropic Particles on Nonplanar Interfaces. *Langmuir* **2008**, *24*, 9302–9307.
- (37) Lewandowski, E. P.; Bernate, J. A.; Tseng, A.; Searson, P. C.; Stebe, K. J. Oriented Assembly of Anisotropic Particles by Capillary Interactions. *Soft Matter* **2009**, *5*, 886–890.
- (38) Lewandowski, E. P.; Cavallaro, M.; Botto, L.; Bernate, J. C.; Garbin, V.; Stebe, K. J. Orientation and Self-Assembly of Cylindrical Particles by Anisotropic Capillary Interactions. *Langmuir* **2010**, *26*, 15142–15154.
- (39) Lin, Y.; Skaff, H.; Emrick, T.; Dinsmore, A. D.; Russell, T. P. Nanoparticle Assembly and Transport at Liquid-Liquid Interfaces. *Science* **2003**, *299*, 226–229.
- (40) Binks, B. P.; Fletcher, P. D. I. Particles Adsorbed at the Oil-Water Interface: A Theoretical Comparison between Spheres of Uniform Wettability and Janus Particles. *Langmuir* **2001**, *17*, 4708–4710.
- (41) Cheung, D. L.; Bon, S. A. F. Stability of Janus Nanoparticles at Fluid Interfaces. *Soft Matter* **2009**, *5*, 3969–3976.
- (42) Jiang, S.; Granick, S. Janus Balance of Amphiphilic Colloidal Particles. *J. Chem. Phys.* **2007**, *127*, 161102–161104.
- (43) Hirose, Y.; Komura, S.; Nonomura, Y. Adsorption of Janus Particles to Curved Interfaces. *J. Chem. Phys.* **2007**, *127*, 054707–054712.
- (44) Cheung, D. L.; Bon, S. A. F. Interaction of Nanoparticles with Ideal Liquid-Liquid Interfaces. *Phys. Rev. Lett.* **2009**, *102*, 066103–066106.
- (45) Park, B. J.; Brugarolas, T.; Lee, D. Janus Particles at an Oil-Water Interface. *Soft Matter* **2011**, *7*, 6413–6417.
- (46) Park, B. J.; Furst, E. M. Fabrication of Unusual Asymmetric Colloids at an Oil–Water Interface. *Langmuir* **2010**, *26*, 10406–10410.
- (47) Park, B. J.; Lee, D. Equilibrium Orientation of Nonspherical Janus Particles at Fluid–Fluid Interfaces. *ACS Nano* **2011**, *6*, 782–790.
- (48) Casagrande, C.; Fabre, P.; Raphaël, E.; Veyssié, M. "Janus Beads": Realization and Behaviour at Water/Oil Interfaces. *EPL* **1989**, *9*, 251–255.
- (49) Jiang, S.; Granick, S. Controlling the Geometry (Janus Balance) of Amphiphilic Colloidal Particles. *Langmuir* **2008**, *24*, 2438–2445.
- (50) Zhang, Z.; Pfeleiderer, P.; Schofield, A. B.; Clasen, C.; Vermant, J. Synthesis and Directed Self-Assembly of Patterned Anisometric Polymeric Particles. *J. Am. Chem. Soc.* **2011**, *133*, 392–395.
- (51) Grzelczak, M.; Vermant, J.; Furst, E. M.; Liz-Marzán, L. M. Directed Self-Assembly of Nanoparticles. *ACS Nano* **2010**, *4*, 3591–3605.
- (52) Morgan, A. R.; Ballard, N.; Rochford, L. A.; Nurumbetov, G.; Skelton, T. S.; Bon, S. A. F. Understanding the Multiple Orientations of Isolated Superellipsoidal Hematite Particles at the Oil-Water Interface. *Soft Matter* **2013**, *9*, 487–491.
- (53) Meng, X.; Guan, Y.; Zhang, Z.; Qiu, D. Fabrication of a Composite Colloidal Particle with Unusual Janus Structure as a High-Performance Solid Emulsifier. *Langmuir* **2012**, *28*, 12472–12478.
- (54) Kraft, D. J.; Ni, R.; Smallegange, F.; Hermes, M.; Yoon, K.; Weitz, D. A.; van Blaaderen, A.; Groenewold, J.; Dijkstra, M.; Kegel, W. K. Surface Roughness Directed Self-Assembly of Patchy Particles into Colloidal Micelles. *Proc. Natl. Acad. Sci. U. S. A.* **2012**, *109*, 10787–10792.
- (55) Ayeward, R. Can Janus Particles Give Thermodynamically Stable Pickering Emulsions? *Soft Matter* **2012**, *8*, 5233–5240.
- (56) Erhardt, R.; Böker, A.; Zettl, H.; Kaya, H.; Pyckhout-Hintzen, W.; Krausch, G.; Abetz, V.; Müller, A. H. E. Janus Micelles. *Macromolecules* **2001**, *34*, 1069–1075.
- (57) Walther, A.; Drechsler, M.; Rosenfeldt, S.; Harnau, L.; Ballauff, M.; Abetz, V.; Müller, A. H. E. Self-Assembly of Janus Cylinders into Hierarchical Superstructures. *J. Am. Chem. Soc.* **2009**, *131*, 4720–4728.
- (58) Kutuzov, S.; He, J.; Tangirala, R.; Emrick, T.; Russell, T. P.; Böker, A. On the Kinetics of Nanoparticle Self-Assembly at Liquid/Liquid Interfaces. *Phys. Chem. Chem. Phys.* **2007**, *9*, 6351–6258.
- (59) de Graaf, J.; Dijkstra, M.; van Roij, R. Triangular Tessellation Scheme for the Adsorption Free Energy at the Liquid-Liquid Interface: Towards Nonconvex Patterned Colloids. *Phys. Rev. E* **2009**, *80*, 051405–051423.
- (60) Andala, D. M.; Shin, S. H. R.; Lee, H.-Y.; Bishop, K. J. M. Templated Synthesis of Amphiphilic Nanoparticles at the Liquid–Liquid Interface. *ACS Nano* **2012**, *6*, 1044–1050.